Impedance and initial magnetic permeability of gadolinium

G. L. F. Fraga, P. Pureur, and L. P. Cardoso

Citation: Journal of Applied Physics **107**, 053909 (2010); doi: 10.1063/1.3288696
View online: http://dx.doi.org/10.1063/1.3288696
View Table of Contents: http://scitation.aip.org/content/aip/journal/jap/107/5?ver=pdfcov
Published by the AIP Publishing

Impedance and initial magnetic permeability of gadolinium

G. L. F. Fraga,[1,a)] P. Pureur,[1] and L. P. Cardoso[2]
[1]*Instituto de Física, Universidade Federal do Rio Grande do Sul (UFRGS), 91501-970 Porto Alegre, RS, Brazil*
[2]*Instituto de Física Gleb Wataghin, Universidade Estadual de Campinas, 13083-970 Campinas, SP, Brazil*

(Received 14 July 2009; accepted 10 December 2009; published online 5 March 2010)

In the present work we report on measurements of the complex impedance and the magnetoimpedance of a textured sample of gadolinium metal. The preferential *c -axis* orientation of the Gd hexagonal structure is perpendicular to the long axis of the sample. From the experimental data, the complex initial magnetic permeability, $\mu=\mu'+i\mu''$, was obtained as a function of temperature and frequency of the ac exciting current. We have found that the results for $\mu'(T)$ below the spin reorientation temperature may be described as a power law of the reduced temperature $t=1-T/T_{SR}$, where T_{SR} is the spin reorientation temperature. This behavior suggests that a genuine phase transition occurs at T_{SR}. Although the impedance displays a weak anomaly at the Curie temperature, T_C, magnetic measurements indicate that the ferromagnetic response of Gd extends up to this critical point. Thus, two different phases characterizes the cooperative magnetic state of this metal. The frequency dependent results for μ' and μ'' were fitted to a modified Debye formula and the obtained parameters allow us to discriminate between the contributions from domain-wall motion and from magnetization rotation. We obtain that the dynamical properties of the domain walls in Gd are governed by a broad distribution of frequencies whose average value diverge at T_{SR}. The isothermal magnetoimpedance measurements in temperatures smaller than T_{SR} show an interesting plateau at low dc applied fields. This plateau is limited by a characteristic field H_K whose magnitude decreases rapidly to nearly zero at T_{SR}, giving further support for the phase transition scenario at this temperature. © *2010 American Institute of Physics*. [doi:10.1063/1.3288696]

I. INTRODUCTION

Gadolinium is a heavy-earth element that crystallizes into the hexagonal close packet structure. The seven unpaired electrons in its $4f$ electron shell are largely responsible for the atomic magnetic moment of $7.12\mu_B$, as determined from magnetization measurements in the ferromagnetic phase.[1] An effective Gd moment of $7.98\mu_B$ was obtained from susceptibility measurements in the paramagnetic phase.[2] The localized spins of the almost spherically symmetrical Gd^{3+} ions are coupled to each other via the isotropic RKKY interaction so that Gd metal is often described as representative of an ideal Heisenberg ferromagnet at low temperatures.[3] The thermal and magnetic properties of Gd have been extensively studied. The heat capacity shows a pronounced maximum at $T_C=293$ K, that signals the paraferromagnetic transition.[4,5] However, the magnetic susceptibility of some samples does not exhibit a divergence at this temperature but shows a sharp maximum at a characteristic temperature $T_{SR}\sim 230$ K.[6] Belov and Ped'ko[7] observed this effect four decades ago and proposed that Gd orders into a helical-antiferromagnetic phase in the range between T_{SR} and T_C. According to their observations and interpretation, the helical-AF order is destroyed upon applying a magnetic field with magnitude above a few Oersted. Contrasting with this model, neutron diffraction studies do not reveal the line satellites characteristic of helical spin structure and support the view that Gd is indeed a collinear ferromagnetic system below T_C.[8,9] Moreover, neutron diffraction experiments also show that just below T_C the magnetic moments are oriented parallel to the *c -axis* of the hexagonal structure. However, below T_{SR} the moments are progressively tilted away from this orientation by a temperature dependent angle. The characteristic temperature T_{SR} is presently recognized as a spin reorientation temperature.

The magnetic state of Gd just below room temperature has been a subject of controversy until recently. Coey *et al.*[6] studied the complex ac susceptibily of single crystals having the *c*-axis oriented either parallel or perpendicullar to the excitation field. These authors claim that in both cases the internal susceptibility (corrected for the demagnetizing effect) does not diverge at T_C. In spite of growing steadily below this temperature, the susceptibilty attains the demagnetization-limited value when the temperature is decreased to T_{SR}, indicating that a fully ferromagnetic spontaneous magnetization only develops below this temperature. Based on this fact, a *c*-axis modulated spin structure, analogous to that found in erbium, was suggested to describe the magnetically ordered state of Gd between T_C and T_{SR}. On the other hand, Kaul and Srinath[10] refuted this interpretation with basis on detailed ac susceptibility and low-field magnetization measurements in high purity single crystals that could be oriented with the *c*-axis either perpendicular or parallel to the probing field. Kaul and Srinath[10] concluded that Gd is indeed a normal uniaxial ferromagnet between T_C and T_{SR}. In particular, they observed that the characteristic anomaly in the ac susceptibility at T_C is absent when the oscillating field is applied along the *c*-axis of a needle-

a)Electronic mail: fraga@if.ufrgs.br.

shaped sample (as in the experiment of Coey *et al.*[6]). Kaul and Srinath[10] suggest that the growth process produces a sinuosity of the *c*-axis orientation along the crystal that simulates a helical spin structure with variable cone angle. This extrinsic effect would prevent the susceptibility from attaining the limit imposed by the demagnetization effect in temperatures between T_{SR} and T_C.

Below the spin-reorientation temperature, the spontaneous magnetization and the ac susceptibility of Gd show rather complex temperature dependences.[2,10] When the temperature decreases, the cone angle θ between the magnetic moment and the *c*-axis increases until a maximum value $\theta = 65°$ is reached near $T^* = 190$ K. This angle decreases to 32° at low temperatures,[8] where the magnetization has been found to follow a $T^{3/2}$ law.[1]

The anisotropy constants related to the magnetocrystalline energy $E_K = K_1 \sin^2\theta + K_2 \sin^4\theta$ were determined from torque measurements.[11] Both K_1 and K_2 behave quite particularly in the temperature range near T_{SR}. The anisotropy constant K_2 is positive in low temperatures, decreases continuously upon increasing T and vanishes at T_{SR}. The constant K_1 is negative in low temperatures, reverses sign at T_{SR} and becomes positive but very small up to 320 K, where it goes to zero. Curiously, exactly at T_{SR} both constants are zero and the system is perfectly isotropic. To the best of our knowledge, Gd is the only ferromagnetic material whose anisotropy constants show this peculiar behavior.

In this work we present a study of the magnetic properties of a bulk Gd textured sample using impedance experiments. As pointed out in a previous paper,[12] impedance measurements are useful to study the critical phenomenology and dynamic properties of domain walls in soft magnetic materials. Indeed, certain magnetic phase transitions generate intrinsic impedance effect below T_C that may be quite strong.[13] Impedance experiments have also been used to study magnetic transitions in nanocrystalline soft magnetic alloys[14] and were employed as an auxiliary experimental technique to detect weak-order magnetic or structural transitions.[15] The impedance $Z(\omega)$ is the response function of a conductor submitted to an alternate electric current $I(\omega)$ so that $V(\omega) = Z(\omega)I(\omega)$, where $V(\omega)$ is the voltage drop between two points at the surface of the sample. The impedance is a complex property that may be written as $Z(\omega) = R(\omega) + iX(\omega)$ where $R(\omega)$ is the electrical resistance and $X(\omega)$ is the reactance. When the sample is magnetic, the ac current magnetizes circumferentially the material. In this case the impedance depends not only on the sample's shape and the frequency of the probe current but also is a function of the magnetic permeability μ of the material.[16] When the magnetic permeability is strongly dependent on the external field, giant magnetoimpedance effects may be observed.[17] Impedanciometry has some advantages when compared to other experimental methods to study magnetic conductors. In addition to the simplicity of the technique, the demagnetizing effects do not play an important role due to the circumferential character of the exciting magnetic field. Moreover, this field is rather small. For a cylindrical sample of 1 mm diameter that carries an electrical current of 20 mA, the self-field attains the maximum value of $\mu_0 H = 40\ \mu T$ at the sample's surface. Consequently, the studied system remain near its magnetic ground state. An obvious disavantage is that the magnetic field produced by the ac current is not homogeneous inside the sample.

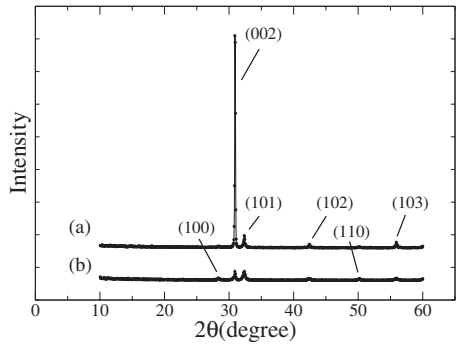

FIG. 1. XRD patterns at room temperature for incidence on two mutually perpendicular surfaces of the sample. The spectrum obtained when the radiation incides on a face perpendicular to the *c*-axis shows a much larger ratio for the amplitudes between the (002) and (101) lines.

The impedance of Gd was measured as a function of temperature and frequency. In some experiments a dc magnetic field was applied parallel to the probe current. Circumferential contribution to the initial magnetic permeability, $\mu(\omega,T) = \mu'(\omega,T) + i\mu''(\omega,T)$, could be obtained from the Z measurements. The real and imaginary parts of the magnetic permeability show the Hopkinson maximum. However, both components are peaked at a temperature nearly below T_{SR} and just a faint anomaly is seen at T_C. Below T_{SR}, the permeability behaves as a power law of the reduced temperature $t = 1 - T/T_{SR}$, suggesting that a phase transition underlies the spin-reorientation phenomenon in Gd.

Impedance measurements as functions of temperature in two different frequencies were performed previously before in a polycristalline Gd sample.[15] No attempt was made to discriminate the real and the imaginary parts of Z in this experiments.

II. EXPERIMENTS

A Gd sample with 99.9% purity with respect to metallic atoms was cut from a highly *c*-axis textured piece by spark erosion. The sample has the form of a parallelepiped with dimensions $1 \times 1 \times 14$ mm^3. The basal plane of the hexagonal crystallites was preferentially oriented parallel to opposite faces of the parallelepiped so that the *c*-axis points perpendicular to the long axis of the sample. Figure 1 compares the x-ray diffraction patterns obtained when the radiation incides on the lateral faces perpendicular or parallel to the *c*-axis preferential orientation. The large difference observed in the ratio between the amplitudes of the (002) and (101) lines in the two diffractograms reveals the significant bulk texturization of the sample.

Magnetization measurements of a small piece of the same Gd sample were performed along and perpendicular to the *c*-axis. A superconducting quantum interference device magnetic properties measuring system from Quantum Design was used in the dc mode for performing these experiments. Results are shown in Fig. 2, which look quite similar to those reported by Kaul *et al.*[10] for a single crystal sample.

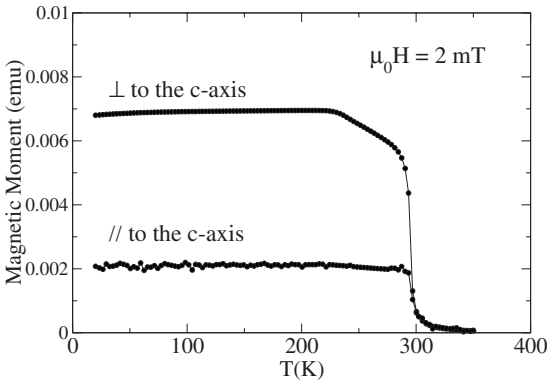

FIG. 2. Temperature dependence of the magnetization obtained when the external field is apllied parallel and perpendicular to the preferential *c*-axis orientation.

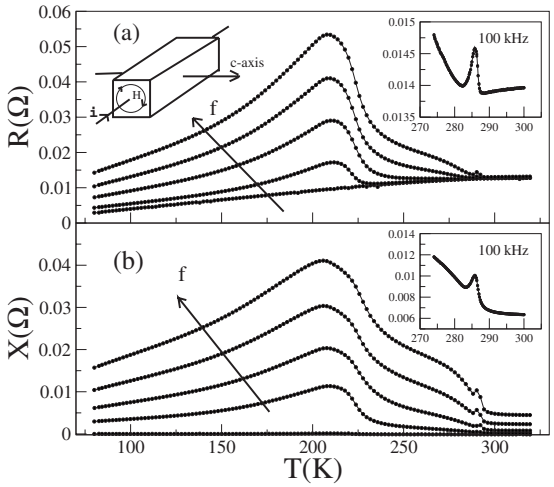

FIG. 3. (a) In-phase resistive and (b) out-of-phase reactive components of the impedance vs temperature for Gd at several frequencies. From bottom to top, in both panels, the curves were obtained with frequencies: 50 Hz, 5 kHz, 20 kHz, 50 kHz, and 100 kHz. The amplitude of the ac current is 20 mA. The solid lines are guides for the eyes The inset shows in more details the results at 100 kHz near T_c. The inset in the top left corner of panel (a) shows the sample and current configuration adopted in our impedance measurements.

When the field is applied along the *c*-axis, the magnetization attains the demagnetizing limit just below T_C, whereas for fields parallel to the basal plane the demagnetizing limit is reached only at T_{SR}.[10] Results in Fig. 2 confirm the highly textured microstructure of our sample. From these measurements, we estimate that $T_C = 293$ K, in agreement with previous determinations.[4,5]

Impedance measurements were carried out with a home made apparatus based on a four-contacts ac technique that employs a dual phase lock-in amplifier as the signal detector. Low Ohmic electrical contacts were made with silver paint on one of the large sample surfaces. The voltage leads were placed nearly 10 mm apart. The current was supplied by a rf generator operating on a sinusoidal mode, with frequency varying between 25 Hz and 100 kHz and fixed rms amplitude of 20 mA. A 50 Ω resistor was placed in series with the sample in order to achieve the best impedance matching with the special cryogenic coaxial cables (Lake Shore, Coax Cable) used to connect the sample to the measuring equipment. As the resistance of the sample is very small, the current remains constant during the experiments. In order to precisely separate the in-phase (resistive) and out-of-phase (reactive) components of the impedance, the voltage drop across a noninductive resistor was used as a reference signal to the lock-in amplifier. A carbon-glass resistor was used as the temperature sensor. Magnetoimpedance measurements were performed by applying a dc magnetic field between -0.05 and $+0.05T$ parallel to the exciting current.

III. RESULTS AND DISCUSSION

A. Impedance and magnetic permeability versus temperature

Measurements of the resistive and reactive components of the impedance as a function of the temperature in several frequencies are shown in Fig. 3. The insets in upper left corner of Fig. 3(a) shows the experimental configuration adopted in our impedance measuments. The probe current is applied parallel to the hexagonal atomic planes so that the azimutal driving field has components both parallel and perpendicular to the *c*-axis. The impedance results shown in Fig. 3 look significantly more complex than those observed in soft and isotropic ferromagnetic systems. Contrasting with results in the Heusler compounds Pd_2MnSn and Pd_2MnSb studied in Ref. 12 only a faint peaked anomaly is observed closely below T_C in both the real and imaginary impedance components. The insets in the upper right corner of both panels in Fig. 3 magnify the results near T_C for the frequency of 100 kHz, showing the occurrence of weak maxima signaling the para-ferromagnetic phase transition. A steep increase in both impedance components occurs when the temperature is decreased below 230 K, approximately. After attaining a round maximum around 210 K the impedance components decrease steadily when the temperature is further decreased. This overall behavior is preserved when the frequency of the ac current increases but with enhanced impedance magnitudes, as depicted in Fig. 3.

In the quasistatic regime the complex impedance for a cylindrical conductor of diameter $2a$ and electrical resistance R_{dc} is given by

$$Z = R_{dc} ka \frac{J_0(ka)}{2J_1(ka)}, \tag{1}$$

where the J_n are Bessel functions of the first kind and $k = (1+i)/\delta$. The skin depth parameter, δ, characterizes the radial decay of the current density inside the conductor and is written as

$$\delta = \left(\frac{\rho}{\pi f \mu \mu_0} \right)^{1/2}, \tag{2}$$

where ρ is the dc electrical resistivity and μ_0 is the vacuum permeability. Equation (1) comes from the solution of the Maxwell's equations when ac electrical and magnetic fields are considered inside the cylindrical conductor.[16]

A computational procedure was used to extract the initial magnetic permeability from the impedance results shown in Fig. 3. Details of this procedure can be found in Ref. 12. Figure 4 shows μ' and μ'' extracted from the analysis of the

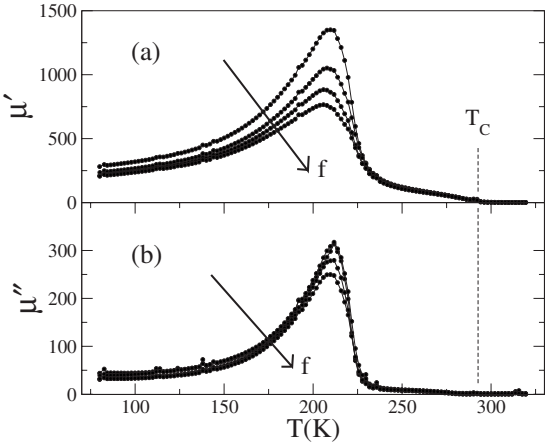

FIG. 4. Real (a) and imaginary (b) components of the complex magnetic permeability vs temperature for Gd at several frequencies. From bottom to top, in both panels, the curves correspond to 100, 50, 20, and 5 kHz. The amplitude of the ac current is 20 mA. The solid lines are guides for the eyes.

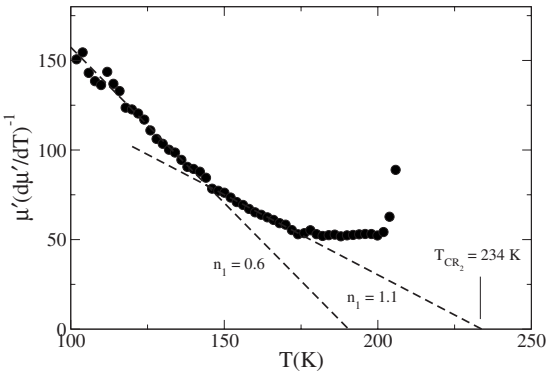

FIG. 5. Kouvel–Fisher plot for the real component μ' measured at 5 kHz.

results in Fig. 3 as functions of the temperature in the different fixed frequencies. One should note that Eqs. (1) and (2) were deduced for isotropic materials, which is not the case of Gd. However, in our experiments the circumferential field has components both parallel and perpendicular to the *c*-axis. Thus, the permeability deduced from Eq. (2) may be viewed as an average between axial and planar components.

Both the real and imaginary components of the magnetic permeability show a pronounced Hopkinson maximum at 210 K for all studied frequencies. This is in contrast with observations in most ferromagnetic materials, where the Hopkinson effect[18] occurs nearly below T_C. The amplitude of this maximum is a decreasing function of the frequency. The magnitude of the dissipative component μ'' is significantly smaller than that of its real counterpart. Above 225 K the permeability is weakly frequency dependent. The results in Fig. 4 do not reveal a clear divergence at T_C. However faint anomalies are observable closely below this temperature in both μ' and μ'' that are reminiscent of the maxima shown in the insets of Fig. 3. We believe that the permeability does not show a strong divergent behavior at T_C because of the particular configuration of our sample. The current is applied perpendicular to the *c*-axis, that is the *easy magnetization* axis in temperatures between T_{SR} and T_C. Thus, the magnetic moments as well the circumferential self-magnetic field lie preferentially on a plane perpendicular to the long sample's axis. The self-field is not quite effective to polarize the moments under these circumstances and the transverse magnetic susceptibility of our sample is expected to be small in this temperature region, in qualitative agreement with results Fig. 4. We notice that a similar effect occurs in amorphous alloys having circumferential anisotropy, where the contribution of spin polarization to the transverse magnetic permeability is essentially zero in the weak field limit.[19]

Near a magnetic phase transition, the enhancement of μ is often attributed to a decrease in the magnetocrystalline anisotropy that makes easier both the motion of domain-walls and rotation of the magnetization. The enhancement of spin polarization competes with the thermal decrease of the magnetization near the ferro-paramagnetic transition so that a maximum known as the Hopkinson effect is produced in the permeability. Interesting enough, the Hopkinson maximum in Fig. 4 occurs nearly below T_{SR} and not close to T_C, as in simple ferromagnetic systems. We should remind, however, that the anisotropy constants in Gd metal are indeed zero at T_{SR}, and remain zero or very small above this temperature.

Results in soft Heusler ferromagnets[12] suggest that a phase transition involving the domain-wall configuration underlies the Hopkinson effect. A continuous phase transition from Bloch walls to linear walls structure is theoretically expected to occur in the ordered phase of uniaxial ferromagnets.[20] Experimental evidences for such transition were obtained in measurements of the kinectic coefficient of the wall relaxation in anisotropic systems.[21,22]

The magnetic domain structure of Gd crystals at low temperatures is rather complex.[23] Although Lorenz microscopy studies of nanometric foil of Gd do not reveal appreciable modifications of the domain geometry when temperature crosses T_{SR},[24,25] it is conceivable that the domain-wall configuration suffers a major change at this temperature in the bulk metal. We thus investigate the possibility for critical behavior in μ near the Hopkinson maximum.

We assume that, near the spin reorientation temperature, the permeability diverges when T approaches a given critical temperature, T_{CR}, as a power law given by

$$\mu' = At^{-n}, \tag{3}$$

where $t=|1-T/T_{CR}|$, A is a constant amplitude and n is a critical exponent. In Fig. 5 we show a Kouvel–Fisher plot[26] for the real component μ' measured at 5 kHz. The identification of a linear regime in this plot allows the simultaneous identification of the critical temperature and exponent. The critical temperature is given by the intersection of the fitted straight line with the T-axis, whereas $1/n$ is given by the slope of the fitted line. Our results show that in the temperature range below the spin reorientation temperature, μ' may be described by two power laws of t with a crossover at approximately 143 K. The fitting at lower temperatures gives $T_{CR_1}=190$ K and $n_1=0.6\pm0.1$. The power law at the higher temperature region is characterized by $T_{CR_2}=234$ K and $n_2=1.1\pm0.1$ (see Fig. 5). It is remarkable that the extrapolated critical temperature for the regime closer to the spin reorientation temperature is coincident with T_{SR}. This fact goes

along with a previous study in the ferromagnetic compound Pd_2MnSn, where the critical temperature for the diverging permeability near the Hopkinson maximum was found to be the Curie point and not some other temperature related to a domain-wall critical reconfiguration.[12] Thus, the Hopkinson effect in Gd and the power law behavior of the permeability described by Eq. (3) suggest that a phase transition occurs at the spin reorientation temperature. The value found for the n_1 exponent in Fig. 5 is quite high when compared to the one identified in Pd_2MnSn. This might be related to the complexity of magnetic domains and domain walls in Gd near T_{SR}. Also noticeable is the approximate coincidence of T_{CR_2} with the temperature where the cone angle θ attains its maximum value.[8,9,23] Results similar to those shown in Fig. 5 were observed in frequencies up to 20 kHz. In higher frequencies, however, the permeability does not scale as in Eq. (3). This occurs probably because the domain-wall motion, which is responsible for the initial permeability in the low frequency regime, does not follow the exciting field above 20 kHz. We could not fit the permeability results to Eq. (3) in temperatures higher than T_{SR}. The occurrence of a phase transition, probably of second-order, inside the magnetically cooperative state of Gd is a significant fact. This means that an order-parameter characterizing the spin reoriented phase develops below T_{SR}. A natural candidate for this order-parameter is the magnetization component perpendicular to the c-axis since an uniaxial ferromagnetic state with spins pointing along the c-axis is stabilized below the critical point T_C.[27] We notice that the occurrence of a second-order phase transition at T_{SR} was previously considered by others[28] and references therein. Based on specific heat and resistivity results, Salamon and Simons[28] proposed that the transition at T_{SR} is driven by the change of sign in the lowest-order anisotropy energy term. According to their model, however, the transition would be supressed as soon as a magnetic field is applied parallel to the basal plane of the Gd unit cell. This prediction does not agree with the characteristics of the transition revealed in their specific heat mesurements and in our impedance experiments.

B. Impedance and magnetic permeability versus frequency

Measurements of the complex impedance versus frequency were performed in several fixed temperatures. Representative examples of these curves are shown in Fig. 6 for 210 K (ferromagnetic phase) and 320 K (paramagnetic phase). In the paramagnetic phase, the resistance $R_{320\ K}$ is nearly constant in the whole frequency range, whereas the reactance $X_{320\ K}$ is very small at low frequencies then becomes a linearly increasing function of f above 1 kHz. In the ferromagnetic phase, the resistance $R_{210\ K}$ is constant up to $f=1$ kHz, then increases continuously above this value. The reactance $X_{210\ K}$ is much higher than in the paramagnetic phase and increases with the frequency in whole studied range. In high-frequencies, the reactance $X_{210\ K}$ behaves similarly to the resistance.

We may interpret the frequency dependence of the measured Gd impedance with basis on Eqs. (1) and (2). In consequence of the skin depth effect, the effective cross section for the ac electron transport should decrease when the frequency is augmented. In magnetic materials, however, the temperature and frequency dependent permeability also plays an important role. In the paramagnetic phase of our sample $\mu=1$ and we estimate that the skin depth is larger than or comparable to the samples's thickness, even at the highest studied frequencies. Then, the current is uniformly distributed inside the conductor and the real component of Z does not vary with frequency, as indeed shown by the R measurements at $T=320$ K in Fig. 6. In the ferromagnetic phase (results at $T=210$ K), the current distribution is nearly uniform inside the conductor only for frequencies below 1 kHz. Because of the large permeability, the current begins to migrate to the sample's surface when f exceeds 1 kHz, approximately. At $f=100$ kHz the current circulates in a thin layer near the sample's surface. The magnetic field generated by the ac electrical current induces a 90° out-of-phase electric field whose values at the surface determine the inductive voltage V_X across the sample. In the case of an uniformly distributed current, the magnetoinductive effect[29] may be written as $V_X(\omega)=-wL_iI(\omega)$, where L_i is the internal inductance, that depends on the sample's shape and the magnetic permeability. The total voltage is then given by $V_T(\omega)=V_R+iV_X=R_{dc}I(\omega)-iwL_iI(\omega)$, where R_{dc} is the resistance at zero frequency. When the permeability does not play a role, V_X is a linear function of the frequency, as shown by the X results at 320 K in Fig. 6. This linearity is also observed at 210 K for frequencies below $f=1$ kHz.

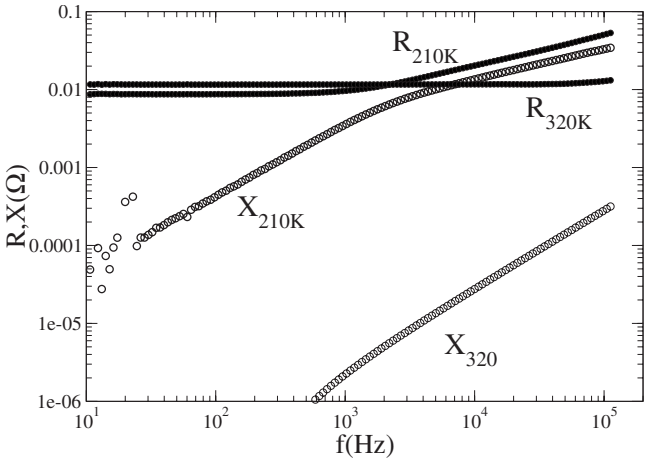

FIG. 6. Frequency dependence of the resistance (filled dots) and reactance (open circles) for Gd at 210 K (ferromagnetic phase) and 320 K (paramagnetic phase). Reactances are corrected for the external contribution. The amplitude of the ac current is 20 mA.

A procedure analogous to the one used for determining μ as a function of temperature was employed to obtain the frequency dependence of the complex magnetic permeability. Figure 7 shows a representative example of μ' and μ'' as functions of the frequency at $T=210$ K. Both components show a relaxational behavior characteristic of domain-wall dynamics. As f increases, the domain-walls become unable to follow the self-field oscillations and damping effects become relevant. This damping is responsible for the decrease of μ', which is accompanied by a maximum of imaginary component, as may be seen in Fig. 7.

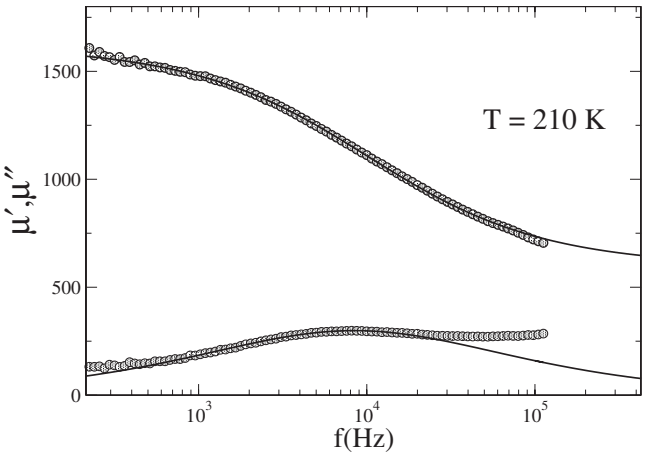

FIG. 7. Frequency dependence of the real (upper curve) and imaginary components of the Gd permeability at 210 K. Full curves are fits to Eqs. (5) and (6).

In the studied frequency range, the magnetic permeability is mainly governed by domain-wall oscillations and magnetization rotations. When the dispersion is relaxational, the complex permeability may be described phenomenologically by the modified Debye formula,[30]

$$\mu = \mu_S + \frac{\mu_T - \mu_S}{1 + (i\omega\bar{\tau})^{1-\alpha}}, \tag{4}$$

where μ_T is the isothermal permeability in the low frequency limit ($\omega\bar{\tau} \ll 1$), μ_S is the adiabatic permeability in the high frequency limit ($\omega\bar{\tau} \gg 1$). The parameter $\alpha(0 \leq \alpha < 1)$ is usually identified to the width of the relaxation time distribution around the average relaxation time $\bar{\tau}$. For $\alpha=0$ one has the original Debye formula, with a single relaxation time.[31] The limit $\alpha=1$ accounts for a distribution of relaxation times having an infinite width. In most experimental cases α is intermediate between the limits 0 and 1. The behavior described by Eq. (4) has been observed in the complex susceptibility of spin glasses,[32] uniaxial ferromagnets,[33] and in Heusler ferromagnets.[12] From Eq. (4), one obtains the frequency dependence of the real and imaginary parts of the complex permeability, that are given by[30]

$$\mu' = \mu_S - \frac{(\mu_T - \mu_S)[1 + (\omega\bar{\tau})^{1-\alpha}\sin(\alpha\pi/2)]}{1 + 2(\omega\bar{\tau})^{1-\alpha}\sin(\alpha\pi/2) + (\omega\bar{\tau})^{2(1-\alpha)}}, \tag{5}$$

$$\mu'' = \frac{(\mu_T - \mu_S)[(\omega\bar{\tau})^{1-\alpha}\cos(\alpha\pi/2)]}{1 + 2(\omega\bar{\tau})^{1-\alpha}\sin(\alpha\pi/2) + (\omega\bar{\tau})^{2(1-\alpha)}}, \tag{6}$$

The continuous curves in Fig. 7 are fits to Eqs. (5) and (6) for the real (upper curve) and imaginary parts of the permeability, respectively. The upturn observed in μ'' at higher frequencies is probably related to surface effects.

Alternatively, the dispersion observed in the complex permeability may be analyzed by plotting μ'' as a function of μ'. This is done in Fig. 8. The solid lines are fits to

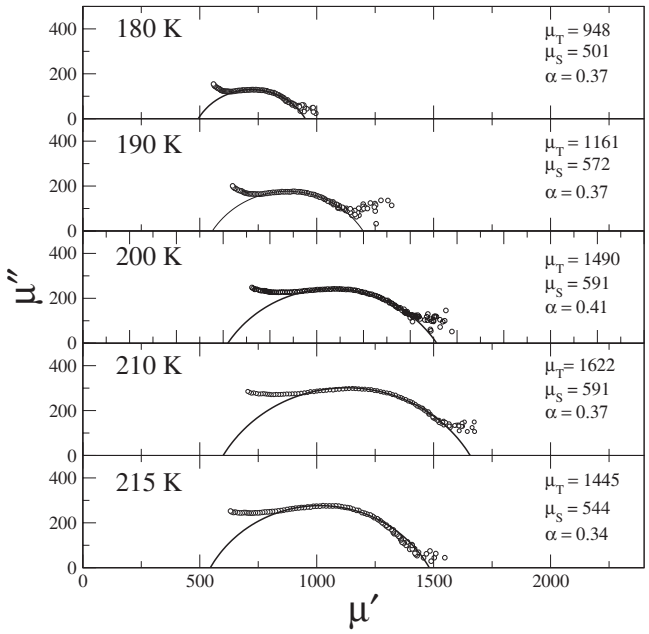

FIG. 8. Argand diagrams for the frequency dependent permeabiliy of Gd at different temperatures below T_{SR}. Frequencies vary from the right (100 Hz) to the left (100 kHz). Continuous lines are fits to Eq. (7).

$$\mu'' = -\frac{\mu_T - \mu_S}{2\tan[(1-\alpha)\pi/2]} + \sqrt{(\mu_T - \mu')(\mu' - \mu_S) + \frac{(\mu_T - \mu_S)^2}{4\tan^2[(1-\alpha)\pi/2]}}. \tag{7}$$

For $\alpha=0$, Eq. (7) represents an arc of a semi-circle in the Argand diagram (or Cole–Cole plot[30]) with its center lying on the real axis.[34] For the data in Fig. 8 we found the distribution parameter $\alpha \sim 0.4$, that does not change noticeably below 215 K. This relatively high value for α indicates the occurrence of a broad distribution of relaxation times, which is not surprising in view of the complexity of the domain configuration in Gd below T_{SR}.[25] The analysis of results in Fig. 8 based on Eq. (7) was systematically used to extract the quantities μ_T, μ_S, and α which were cross-checked with the same quantities obtained from fits like those shown in Fig. 9, that were based on Eq. (5). Those fits also allow the deter-

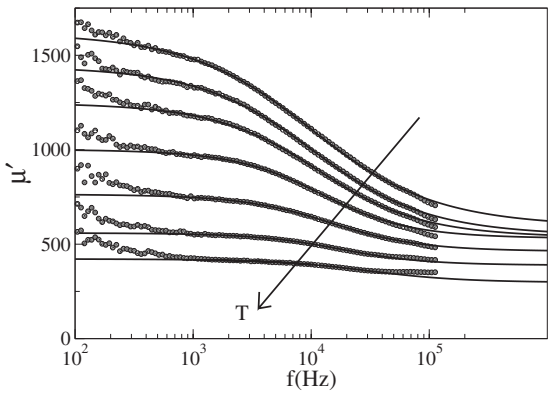

FIG. 9. Frequency dependence of the real component of the complex permeability at several temperatures below T_{SR}. From top to botton, the curves correspond to 210, 215, 217, 219, 221, 223, and 225 K. Full curves are fits to Eq. (5).

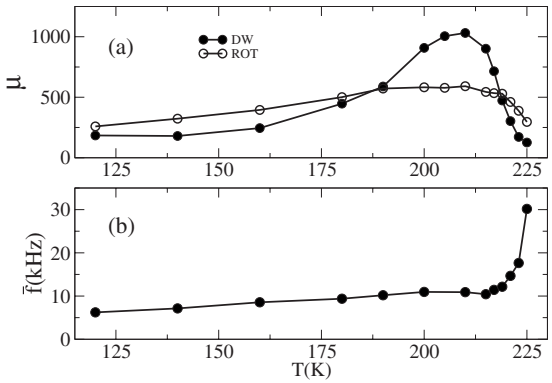

FIG. 10. (a) $\mu_{DW}=\mu_T-\mu_S$ and μ_S vs T contributions to the permeability of Gd and (b) temperature dependence of the average relaxation frequency. These parameters are obtained from fitting the experimental data to Eqs. (5) and (6).The solid lines are guides to the eyes.

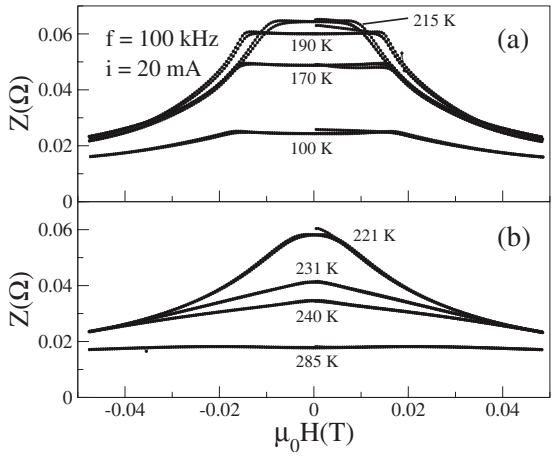

FIG. 11. Impedance at 100 kHz measured as a function of the magnetic field in temperatures (a) below T_{SR} and (b) above T_{SR}.

mination of $\bar{\tau}$. Figure 9 shows representative examples of the real component of μ as a function of the frequency in several temperatures below T_{SR}.

The difference $\mu_{DW}=\mu_T-\mu_S$ is associated to domain-wall motion, whereas μ_S is related to spin rotation in the high-frequency limit.[35–37] Figure 10(a) shows the temperature dependence of μ_{DW} and μ_S. Both μ_{DW} and μ_S increase with temperature up to 210 K, then decrease rapidly near 225 K. According to data in Fig. 10(a), between 190 and 218 K the contribution of the domain-wall motion to the magnetic permeability dominates over the spin rotation term. This result reinforces the interpretation attributing the power law behavior observed in the real component μ' below 230 K to domain-wall dynamics. In panel (b) of Fig. 10 we plot the temperature dependence of the average relaxation frequency $\bar{f}=1/\bar{\tau}$ as obtained from the data in Fig. 9. Clearly, $\bar{f}$ diverges at $T=T_{SR}$, confirming the critical character of the spin-reorientation transition in Gd.

Results above T_{SR} looks qualitatively similar to those shown on Figs. 7 and 9 but detailed analysis is difficult because permeability decreases steeply to very small values a few degrees above T_{SR}

C. Magnetoimpedance

Figures 11(a) and 11(b) show the impedance Z as a function of the external magnetic field applied parallel to the long sample's axis. The frequency of the exciting current is 100 kHz. In order to reset the remnant magnetization, before each of these isotherm measurements, the sample was warmed to 320 K (paramagnetic phase) and cooled down to the measuring temperature in zero magnetic field. The field was then applied and cycled in the sequence: 0 to $+0.05T$, then $+0.05$ to $-0.05T$, and finally -0.05 to $+0.05T$. The isotherms present distinct characteristics depending if they are measured below or above T_{SR}, as shown in Fig. 11(a). Below this temperature, the isotherms display a plateau in low-fields that extends up to a characteristic value $H=\pm H_K$, where a faint impedance maximum may be seen. When the external field exceeds H_K, a strong and negative magnetoimpedance effect becomes observable. This effect becomes progressively larger as T_{SR} is approached from below. Concomitantly, the field H_K decreases and goes to zero at approximately $T=T_{SR}$, as depicted in Fig. 12. Above T_{SR}, the magnetoimpedance does not show the plateau at low applied fields but is nearly linear with H in the studied range, and becomes extremely small when the temperature approaches T_C [see Fig. 11(b)].

The low-field plateaus as in Fig. 11(a) are often observed in magnetoimpedance measurements of ferromagnetic materials.[17,38] A possible explanation of this feature comes from a rearrangement of the domain structure so that the internal field remains zero up to a certain value of the external dc field. According to the "phases" theory by Nèel *et al.*[39] for the magnetization process of a bulk ideal ferromagnet, the demagnetizing field may exactly cancel the external H as far as the global magnetization is kept below a certain threshold. Then, the permeability would maintain its initial value up to a certain characteristic applied field H_K that has also been interpreted as an anisotropy field.[40,41] Its temperature dependence for our Gd sample is shown in Fig. 12. In this figure, one observes that H_K decreases strongly as T approaches T_{SR} from below. Substitution of the value obtained for H_K in $T=150$ K in the expression $K_1=(H_K M_S)/2$,[41] where M_S is the saturation magnetization, allow us to esti-

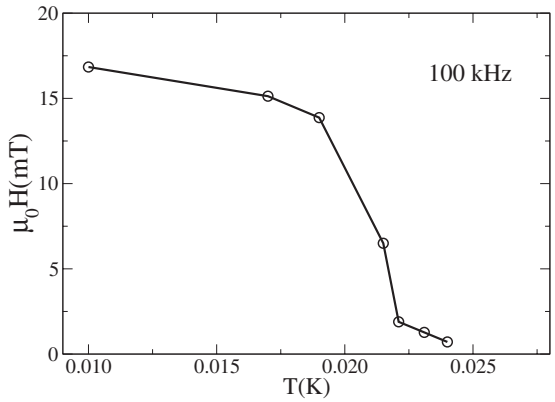

FIG. 12. Magnetic field H_K vs temperature. Solid lines are guides to the eyes.

mate that $K_1=2\times10^5$ erg/cm^3. This 'order of magnitude' estimation is significantly smaller than the value reported by Graham[11] who found $K_1=8\times10^5$ erg/cm^3. We believe that the discrepancy between these values is in part due to our poor estimation of the saturation magnetization and to the fact that our sample is not a true single cristal. Moreover, the characteristic field H_k may not be exactly coincident with the anisotropy field deduced from experiments probing the longitudinal spin component.

Above the spin reorientation temperature, the moments are aligned parallel to the crystallographic *c*-axis. Since the long dimension of our sample is perpendicular to this axis, the longitudinal dc field tilts the spins toward its orientation, producing the linearly field dependent magnetoimpedance observed in Fig. 11(b). In addition, the absence of hysteresis in the magnetoimpedance curves measured above T_{SR} indicates that the domain-wall motion has a minor importance, if any, to describe the permeability of our Gd textured sample in the uniaxial ferromagnetic range between T_{SR} and T_C.

IV. CONCLUSIONS

In this article we present an experimental study on the temperature and frequency dependent impedance of a highly textured Gd sample. Temperatures were varied from values well below the spin reorientation temperature up some degrees above the Curie temperature. Applied frequencies spans the range from 5 to 100 kHz. A computational procedure allowed the extraction of the circumferential initial permeability from the impedance data in the same temperature and frequency ranges. The circumferential permeability shows a pronounced and sharp Hopkinson maximum located close to T_{SR}. Below this temperature, the real part μ' is dominated by domain-wall fluctuations and may be described as a power law of the reduced temperature $1-T/T_{SR}$. This fact strongly suggests that a thermodynamic phase transition occurs at the spin reorientation temperature in the ferromagnetic phase of Gd.

The frequency dependence of both the real and imaginary parts of the magnetic permeability were extensively studied in the ferromagnetic phase of our sample using the modified Debye formula. Relaxational effects were found to be important below T_{SR}. The isothermal and adiabatic contributions to the permeability, as well the relaxation exponent could be obtained from these analyses. We confirmed that the contribution from domain-wall motion is responsible for the critical behavior of μ below T_{SR}. The average inverse relaxation time shows a divergent behavior when the temperature approaches T_{SR} from below, confirming the critical character of the spin reorientation phenomenon in Gd. Impedance was also studied when a weak dc magnetic field was applied parallel to the current orientation.

The low-field magnetoimpedance results reveal the occurrence of low-field plateaus in the temperature range below T_{SR}. These plateaus are limited by a characteristic field H_K that is temperature dependent and nearly vanishes at T_{SR}. Above the spin reorientation temperature, the magnetoimpedance is approximately linear in the longitudinal applied field. As a final conclusion, our impedance measurements in the ferromagnetic phase of Gd are rather compatible with the view that a collinear spin structure with easy axis parallel to the crystallographic *c*-axis occurs in the phase between T_{SR} and T_C. At T_{SR} a transition occurs to a spin reoriented phase where the order-parameter is the magnetization component perpendicular to the *c*-axis.[28] However, further impedance studies in crystals having the *c*-axis parallel to the current orientation are needed to completely elucidate the mechanisms underlying the dynamical behavior of the permeability in the ferromagnetic phase of Gd metal.

ACKNOWLEDGMENTS

This work was partially financed by the PRONEX-FAPERGS/CNPq under Grant No. 04.0938.0.

[1] J. F. Elliott, S. Legvold, and F. H. Spedding, Phys. Rev. **91**, 28 (1953).
[2] H. E. Nigh, S. Legvold, and F. H. Spedding, Phys. Rev. **132**, 1092 (1963).
[3] R. J. Elliott, *Magnetism*, edited by G. T. Rado and H. Suhl (Academic, New York, 1965), Vol. IIA.
[4] M. Griffel, R. E. Skochdopole, and F. H. Spedding, Phys. Rev. **93**, 657 (1954).
[5] S. Dan'kov and A. M. Tishin, Phys. Rev. B **57**, 3478 (1998).
[6] J. M. D. Coey, K. Gallagher, and V. Skumryev, J. Appl. Phys. **87**, 7028 (2000).
[7] K. P. Belov and A. V. Ped'ko, Sov. Phys. JETP **62**, 62 (1962).
[8] G. Will, R. Nathans, and H. A. Alperin, J. Appl. Phys. **35**, 1045 (1964).
[9] J. W. Cable and E. O. Wollan, Phys. Rev. **165**, 733 (1968).
[10] S. N. Kaul and S. Srinath, Phys. Rev. B **62**, 1114 (2000).
[11] J. C. D. Grahm, J. Appl. Phys. **34**, 1341 (1963).
[12] G. L. Ferreira-Fraga, L. A. Borba, and P. Pureur, Phys. Rev. B **74**, 064427 (2006).
[13] G. L. F. Fraga, P. Pureur, and D. E. Brandão, Solid State Commun. **124**, 7 (2002).
[14] C. Gómez-Polo, J. I. Pérez-Landazabal, V. Recarte, M. Vázquez, and A. Hernando, Phys. Rev. B **70**, 094412 (2004).
[15] V. V. Khovailo and T. Abe, J. Appl. Phys. **94**, 2491 (2003).
[16] L. D. Landau and E. M. Lifshitz, *Electrodynamics of the Continuous Media* (Pergamon, Oxford, 1960).
[17] F. L. A. Machado, C. S. Martins, and S. M. Rezende, Phys. Rev. B **51**, 3926 (1995).
[18] J. Hopkinson, Philos. Trans. R. Soc. London **180**, 443 (1889).
[19] D. Atkinson and P. T. Squire, IEEE Trans. Magn. **2264**, 2264 (1997).
[20] L. N. Bulaevski and V. L. Ginzburg, Sov. Phys. JETP **530**, 530 (1964).
[21] J. Kötzler, D. A. Garanin, M. Hartl, and L. Jahn, Phys. Rev. Lett. **71**, 177 (1993).
[22] M. Hartl-Malang, J. Kötzler, and D. A. Garanin, Phys. Rev. B **51**, 8974 (1995).
[23] W. D. Corner and B. K. Tanner, J. Phys. C **627**, 627 (1976).
[24] J. N. Chapman, W. H. McKendrick, R. P. Ferrier, and D. A. Hukin, *International Conference on Rare Earths and Actinides*, 1977 (Whitefriars, Whitefriars, 1978).
[25] W. D. Corner, F. M. Saad, D. W. Jones, and R. G. Jordan, *International Conference on Rare Earths and Actinides* (Whitefriars, Whitefriars, 1978).
[26] J. S. Kouvel and M. E. Fisher, Phys. Rev. **136**, A1626 (1964).
[27] S. Srinath and S. N. Kaul, Phys. Rev. B **59**, 1145 (1999).
[28] M. B. Salamon and D. S. Simmons, Phys. Rev. B **7**, 229 (1973).
[29] K. Mohri, T. Kohzawa, K. Kawashima, H. Yoshida, and L. V. Panina, IEEE Trans. Magn. **28**, 3150 (1992).
[30] K. S. Cole and R. H. Cole, J. Chem. Phys. **9**, 341 (1941).
[31] P. Debye, *Polar Molecules* (Chemical Catalogue Company, New York, 1929).
[32] C. Dekker, A. F. M. Arts, and H. W. de Wijn,A. J. van Duyneveldt, J. A. Mydosh Phys. Rev. B **40**, 11243 (1989).
[33] M. Grahl and J. Kötzler, Z. Phys. B: Condens. Matter **75**, 527 (1989).
[34] D. Huser, A. J. van Duyneveldt, G. J. Nieuwenhuys, and J. A. Mydosh, J. Phys. C **19**, 3697 (1986).
[35] H. J. de Wit and M. Brouha, J. Appl. Phys. **57**, 3560 (1985).
[36] M. T. González, K. L. Garcia, and R. Valenzuela, J. Appl. Phys. **85**, 319 (1999).

[37]M. Carara, M. N. Baibich, and R. L. Sommer, J. Appl. Phys. **88**, 331 (2000).
[38]R. L. Sommer and C. L. Chien, Appl. Phys. Lett. **67**, 857 (1995).
[39]L. Nèel, R. Pauthenet, G. Rimet, and V. S. Giron, J. Appl. Phys. **31**, S27 (1960).
[40]R. L. Sommer and C. L. Chien, Appl. Phys. Lett. **67**, 3346 (1995).
[41]K. R. Pirota, M. Knobel, and C. Gomez-Polo, Phys. Rev. B **320**, 000163 (2002).